Evaluating the Ratio of Electron and Hole Mobilities from a Single Bulk Sample Using Photo-Seebeck Effect

Zhenyu Pan[a], Zheng Zhu[a], Fan Yang[b], Ayaskanta Sahu[c], Jeffrey J. Urban[d*], and Heng Wang[a*]

[a]Department of Mechanical, Materials, and Aerospace Engineering, Illinois Institute of Technology, Chicago, IL 60616, USA. E-mail: heng.wang@iit.edu

[b]Department of Mechanical Engineering, Stevens Institute of Technology, Hoboken, NJ 07030, USA.

[c]Department of Chemical and Biomolecular Engineering, New York University, Brooklyn, NY 11201, USA.

[d]The Molecular Foundry, Lawrence Berkeley National Laboratory, Berkeley, CA 94720, USA.E-mail: jjurban@lbl.gov

When a semiconductor is under photoexcitation, the voltage response to a temperature gradient is the photo-Seebeck effect. Here we study this effect, focusing on the contribution from transport of photo-excited carriers. We demonstrate that by combining photo-Seebeck with photoconductivity measurements, one can determine the ratio between electron and hole mobilities, and hence both of them when one is known. This is found for the case of defect-free samples, where no detail on the absorbance, carrier lifetime or recombination is necessary. Our method reported here does not require chemical doping, which could introduce defects and is often not feasible. It applies to both thin film and bulk samples. Experiment wise, photo-Seebeck effect is relatively easy to implement, or added to existing systems. In a broader context, for semiconductors with significant influence from defects, our result suggests that the photo-Seebeck behavior can still be understood. In this case

another photo-transport property is necessary, in order to identify the mobilities of carriers and information regarding the defects. This framework integrates the information from photoexcitation and thermal gradients to provide a general method to determine fundamental electronic properties of materials.

Keywords: Carrier mobilities; Seebeck effect; Carrier transport; Thermoelectric properties

1. Introduction

Thermoelectric transport phenomena determine a semiconductor's potential for use in thermoelectric devices, which are extensively studied for applications in power generation and solid state cooling[1]. Meanwhile, material properties such as the Seebeck coefficient are widely studied in semiconductor research. The Seebeck coefficient (*S*) is the proportionality between the open circuit voltage and the temperature difference across a conductor. It can be used to determine the carrier type. Its temperature dependence can be used to determine the bandgap E_g. The carrier density dependence of *S* (Pisarenko relation[2]) is used[3] to determine carrier effective mass m^*, while the dependence of *S* on conductivity ($\ln\sigma$) formulated by G. Jonker in 1968,[4] provides information on the weighed mobility $\mu_0 m^{*3/2}$ (μ_0 is mobility at low doping levels). Plenty of examples exist in the literature of thermoelectric material research[5-9].

Thermoelectric responses can be evaluated when a semiconductor is under photon illumination. Take Seebeck effect as an example: a homogeneous semiconductor is illuminated by uniform, continuous light. A steady temperature gradient is applied perpendicular to the illumination. An open circuit voltage is observed across the

semiconductor along this direction, which is proportional to the temperature difference. Seebeck coefficient determined under illuminated conditions can be different from the un-illuminated case, since photons can generate free carriers in the semiconductor which contribute to transport properties alongside the inherent, thermal carriers.

While thermoelectric properties have been studied widely, the photo-thermoelectric properties of a semiconductor have received little attention. Actually, the photo-Seebeck effect has been known for decades. For example, in the 1970s, R. Bube and his group studied the Seebeck coefficients of bulk GaAs and Si, as well as CdS films under photon illumination[10, 11]. Later Terazaki and his group reported Seebeck coefficients in bulk ZnO[12] PbO[13], and[14] $PbCr_2O_5$ illuminated with photon of different wavelengths. As important as these works are, they lack adequate analysis and interpretation of results, no practical application was demonstrated either. In recent years, the term "photothermoelectric effect" is often used in literature for a related yet different phenomenon: the detection of photocurrent under localized illumination on devices made of graphene[15, 16] or other low dimensional materials[17-20], where the temperature gradients were generated by focused light beams. This is not to be confused with effects discussed here.

In this work, we studied the photo-Seebeck effect in two distinctively different semiconductors: single-crystalline Si and polycrystalline Se. We demonstrate that with proper measurement strategy, photo-Seebeck coefficient of semiconductors due to photo-excited carrier transport can be evaluated and its dependence on illumination intensity can be interpreted. When combined with photo-conductivity measurements, it will allow researchers to evaluate mobilities for both types of carriers, which are

critical parameters for almost all applications of semiconductors. Using regular approach, the semiconductor has to be doped both n-type and p-type using suitable doping strategies, which is often not straightforward, sometimes even unachievable. With photo-Seebeck measurements, the carrier mobilities can be determined from a single, intrinsic sample. As no chemical doping is necessary, the potential impact on mobilities from doping induced defects can be avoided as well. Lastly, our method can be applied to both thin films and bulk samples. The use of bulks samples presents another advantage as high quality sample synthesis sometimes requires less effort for bulks.

The measurement configurations used in this study are illustrated in Fig. 1. Photo-conductivity measurements are performed using standard four-lead method on a bar sample, with the part of sample between two voltage probes illuminated. For photo-Seebeck effect, masking the contact area is important, the masking method (as the ones illustrated) should be able to block most of stray/scattered light from getting to the contact areas. Shadow masks were found not sufficient.

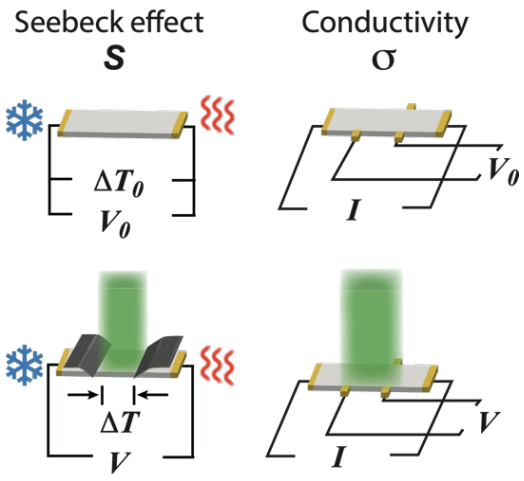

Fig. 1 Illustrations of how photo-Seebeck effect and photoconductivity due to photo-excited carriers are evaluated. Masks are used for photo-Seebeck measurement to remove photovoltaic effect at contacts. Measured quantity $(V\text{-}V_0)/\Delta T$ reflects the difference between photo-Seebeck coefficient and Seebeck coefficient at dark.

When bulk samples are used, photo-excited carriers can only populate a thin layer near the surface whereas a large portion of the sample remains unaffected by illumination. The measured properties are contributions from both, resembling a parallel circuit. As a result, the changes in measured Seebeck coefficient from bulk samples are usually very small (this is also because electron and hole contributions compensate each other). It is thus preferred to use a lock-in amplifier locked to illumination frequency (via a mechanical chopper), which measures the difference between photo-Seebeck coefficient and corresponding dark value. This approach is used here to study single crystal Si. In more general conditions, its applicability depends on the material's response speed to illumination. semiconductors such as polycrystalline Se have very slow response to illumination changes over several minutes. A slow photo-response is common in semiconductor photoconductors due to the presence of defects, sometimes known as persistent photo-conductivity[21]. If this is the case, continuous illumination has to be used. For Se, we performed Seebeck coefficient measurement using a different AC technique locked to temperature oscillation, which provided better sensitivity than DC method.

In a recent high-profile publication[22]. Photo-Hall effect was used to study carrier mobilities of both types. Photo-Seebeck effect provides an alternative, which is usually easier to implement than photo-Hall effect measurements. In a more general case, the two should be combined to better understand a broader range of photo-sensitive semiconductors.

2. Methods

The Si sample used is a 12.7 mm × 3.31 mm × 0.5 mm bar cut from a commercial wafer (n-type, 2-inch diameter, polished), cleaned by sonicating with acetone, isopropanol, then de-ionized water. Contacts are formed with Ag paste and contact areas were polished to remove the oxide layer. Cu probes are used to make electrical contact with them. Temperatures are read by two miniature K type thermocouples with 1mm diameter junction. The thermocouples are brought into contact with the sample surface using spring force. Thermal paste was used to improve thermal coupling.

The Se sample is prepared by melting elemental Se beads (99.999%) in sealed quartz tubes at 623 K, followed by slow cooling to room temperature at 3K/min. A slab 8.8 mm × 4.3 mm × 0.3 mm is obtained by sanding down a piece of ingot, surface of the slab was polished and finished with 2400 girt polishing paper. Contacts are formed in the same manner as the Si sample. For both samples Ohmic behavior is confirmed with I-V tests.

Photo-conductivities are measured with DC method for both Si and Se, as the changes are much more significant, well above measurement uncertainty.

Illumination is provided by LEDs with wavelengths 780 nm and 565 nm. Light output was collimated into a beam with 8 mm diameter. The photon power intensity was calibrated with a thermopile based photon power sensor. Power density used was between 0.2 mW/cm^2 and 2.7 mW/cm^2.

3. Results

Basic characterization with SEM and XRD are performed for Se (on a different sample from same ingot) and results are shown in Fig. 2. Se crystalized in single-phase, with hexagonal structure, which is its expected room temperature phase. The sample is composed of dense and large grains with sizes on the order of 10 μm indicated by the SEM examination. Although it is a simple, single-element compound, properties of crystalline Se showed considerable variations among different studies. Bandgap of thin film Se was reported[23-25] to be 1.8 and 1.95 eV in different studies. Se is also known to possess the so-called persistent photo-conductance[21, 26, 27], where its conductivity settles very slowly (longer than several minutes) when a steady illumination is turned off. Such behaviour is believed due to defect states and slow transition of trapped charge carriers between them. We monitored the transient

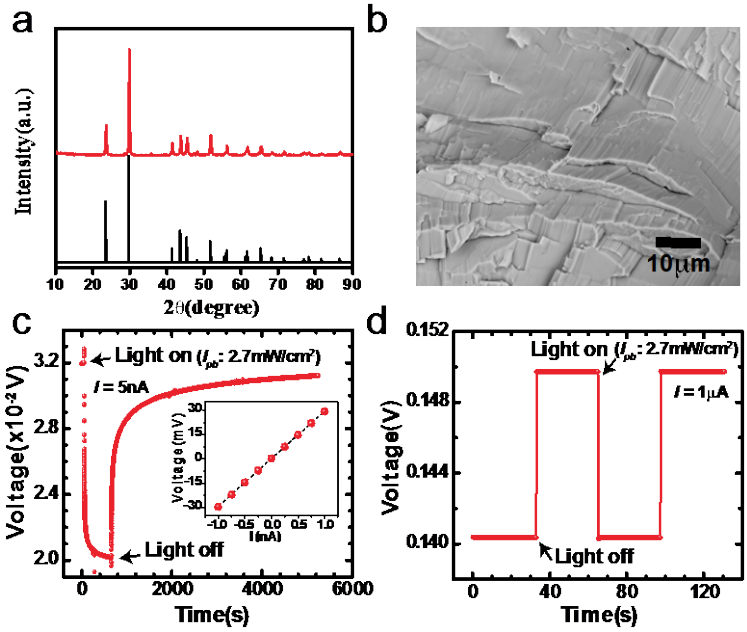

Fig. 2 Sample characterization and photo-response. a) XRD pattern of polycrystalline Se used in this study, revealing a single-phase, hexagonal structure, reference pattern from Pearson's Crystal Data 1632009. b) SEM image of fracture surface of a Se ingot, large elongated grains are as expected for a slow cooled compound with hexagonal lattice. c) and d) Photo-response of Se and Si under 565 nm illumination. Long response time was found in Se due to defect influence. Inset of c) shows Ohmic I-V behaviour from Se.

behaviour of the Se sample as we change illumination conditions between off and maximum, the result is shown in Fig. 2c).

Si is of high quality and the photo-response of the Si sample is found very fast and perfectly linear with photon intensity. No material characterization was performed for Si.

Photo-Seebeck coefficient values depend on measurement strategy very sensitively (Fig. 3a)). This is because of multiple origins of voltages that are proportional to the temperature difference. The most notable one is not due to Seebeck effect from photo-excited carriers, but instead from the photovoltaic effect across metal-semiconductor interfaces. Fig. 3b) shows a comparison of measured "photo-Seebeck coefficients" of the Se sample under different measurement conditions, their key difference is whether the contact areas are blocked from illumination or not. Under both conditions, the voltages change linearly with temperature difference which are

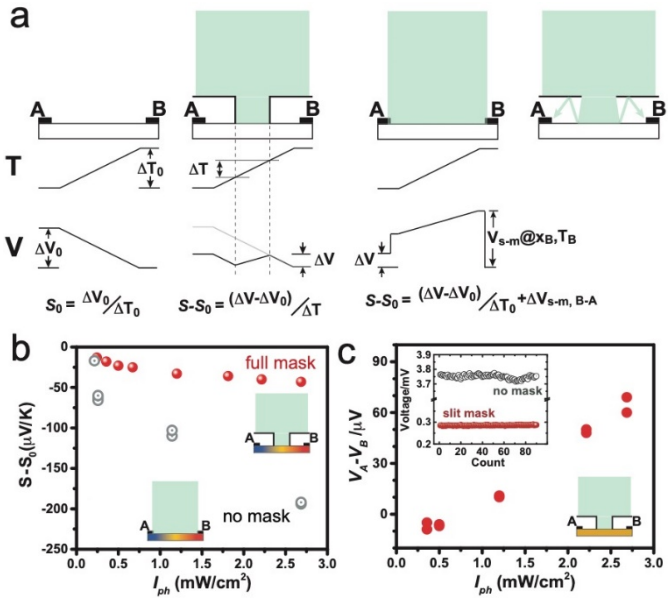

Fig. 3 Illustration of photo-Seebeck measurements under different conditions. a) The temperature and electrical potential profile across a thin film sample under different conditions. For bulk samples this represents the thin surface layer with photo-generation. From left to right: dark, full mask, no mask, and slit mask. With full mask, the voltage between contact "A" and "B" can be used to calculate photo-Seebeck coefficient *S*. When contact area is illuminated, the photo-voltage at semiconductor-metal interface $\Delta V_{s\text{-}m}$ play a more significant role. b) difference between photo-Seebeck coefficient *S* and dark seebeck coefficient S_0 measured in Se as functions of photon intensity (565nm), under different conditions as illustrated. Colours across sample represent temperature gradient. c) voltages measured under isothermal conditions between A and B with different light intensities, with full mask. Colour of sample represents a homogeneous temperature profile. Inset: The same voltage measured under different conditions at I_{ph} = 2.7mW/cm^2. Data obtained from a different sample.

consistent with the definition of Seebeck effect, the apparent “Seebeck coefficients” show a similar trend which decreases with illumination intensity. Nonetheless, it can be seen that the true contribution due to photo-excited carrier transport is fairly small: no more than 4% change based on the dark value (+1250 μV/K). Meanwhile when no intentional masking is applied, we observed a change up to 16%.

Even though the two contacts are made of the same kind of metal, the interfaces are rarely truly identical and perfectly ohmic, thus giving rise to a difference in photovoltaic voltages which can be seen even under isothermal conditions (Fig.3c). As photovoltaic voltages are temperature dependent, an equivalent “Seebeck effect” will be present when the sample is under a temperature gradient. This is reflected in Fig.3b where the change of Seebeck coefficients are much larger when contact areas were illuminated. We chose to remove this effect from further analysis since it heavily depends on the nature of contacts which are hard to control and duplicate, even though it also deserves systematic study. Various masking schemes were experimented such as slits on the optical access window (several millimetres away from sample surface), this led to readings in between those values obtained with and without masking. Fig. 3c) shows the photovoltaic voltages measured across the two contact areas (marked as A and B) under isothermal conditions. With masking method shown in Fig.1 we could block most of scattered light to minimize this voltage (whereas slits or shadow masking would not be sufficient). Complete removal of this bias at $\Delta T=0$ seems unlikely, considering the presence of bulk-photovoltaic effect[28] due to the inevitable inhomogeneity in most materials. Nonetheless, this only has influence on final results through its temperature dependence, which can be further minimized by averaging different parts of a sample.

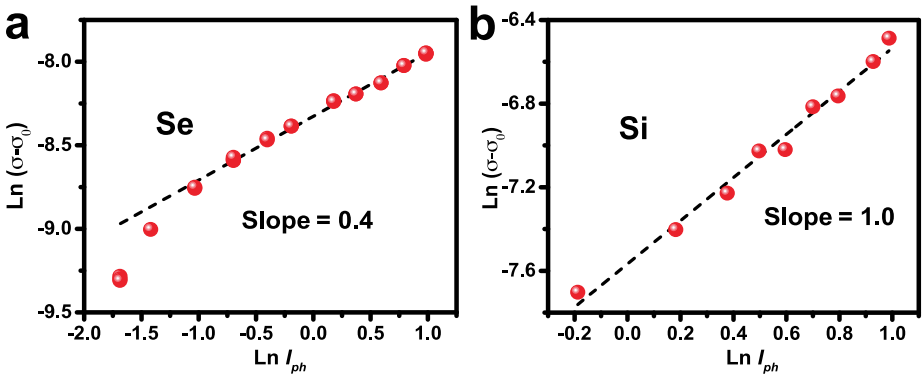

Fig. 4 Photo-conductivity results of Se and Si. a) difference between photo-conductivity σ and dark conductivity σ_0 as a function of photon intensities for Se. b) the same experiment for Si. Different slopes in a) and b) indicate the presence of defects in Se.

The photo-conductivity on the other hand, is not affected by this photovoltaic voltage, as it can be removed by reversing the current direction. From Figure 4a) and 4b) we see the photo-conductivity under 565 nm illumination varies differently with illumination intensity for Si and Se. In Si, a perfectly linear relation is seen which is typical for high-quality, low-defect semiconductors. Se shows a nonlinear, exponential dependence of conductivity on photon intensity (with the exponent less than one), which is also a typical behaviour seen in semiconductors with significant defect influence.

4. Analysis

Photons excite carriers in semiconductors. For common inorganic semiconductors at room temperature and above, the excited species are free carriers. The exact result of photon excitation (or, photon doping) varies under different conditions: As most commonly regarded, photons with energies above the bandgap cause band-to-band excitations, creating electron-hole pairs in equal numbers. The initial relaxation towards band edges can be considered instantaneous, so the excited carriers populate the lowest allowed energy states at the band edge. The electrons will stay for some time before they recombine with holes. This limiting time scale is the (minority) carrier

lifetime, which is long (>10^{-6} *s*) in high quality, photo-sensitive semiconductors[29, 30]. For instance, in Si minority electrons can live up to[31] 1 millisecond. So, carrier distribution can be described by the same Fermi statistics with a quasi-Fermi level. Under continuous illumination, there is a steady number of photon-generated electrons and holes, which is proportional to minority carrier lifetime and illumination intensity.

Photo-transport is thus a standard two-carrier transport problem which we can apply classic transport equations to. Photo-excited carriers are treated in the same manner as for thermal carriers. Even though there is a diffusion process for these carriers towards the inside of the sample, diffusion terms are not considered for transport properties in the perpendicular direction. Also, because transport properties are macroscopic properties of the bulk, surface-state influences can be neglected as well.

In some thin film samples, photo-excited carriers populate throughout the thickness direction with near-uniform distributions. This happens when the sample thickness is smaller than, or comparable with, the optical penetration depth *W* or the carrier diffusion length *L*. Photo-Seebeck behaviour can be easily simulated in this case and an example is presented in Figure 5. Material parameters used for this example are hypothetical but realistic: $m_e^* = m_h^* = 0.3\ m_e$, intrinsic carrier density $n_{h,0} = 1\times10^{12}$ cm^{-3}. Blue dots are for different cases with different mobility ratios between the electrons and holes $\beta = |\mu_e/\mu_h|$. The green line represents regular chemical doping behavior if observed from different samples (assumed n-type).

With chemical doping (neglecting very low doping conditions), the relation between Seebeck coefficient and conductivity (S vs $\ln\sigma$) is called the Jonker plot, which has a

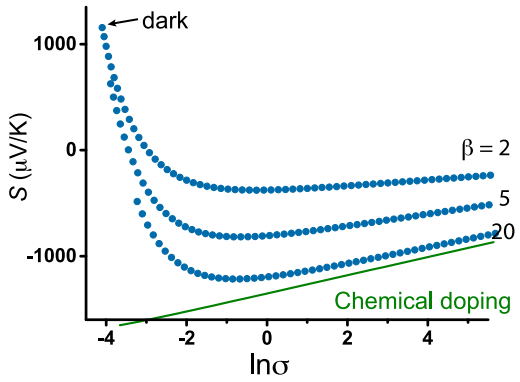

Fig. 5. Simulation of photo-Seebeck analysis. Simulated relations between *S* and lnσ (arbitrary unit) for both conventional chemical doping (n-type) and photon doping, assuming different carrier mobility ratios β.

universal slope (k_B/e) regardless of materials properties. Photo-Seebeck coefficient behave differently: *S* vs lnσ is a different linear relationship when photon intensity is sufficiently high (larger σ). The analytical form of this linear relation is given by Equation 1, the slope is determined by $k_B(\beta -1)/e(\beta +1)$ (detailed derivation will be included in a separate paper, but can be found in ref.[32]). Under lower photon intensities, the relations are no longer linear and extrema (minimum in this case) were reached at certain σ. This minimum can also be expressed analytically[32] and may provide information on the weighed mobilities $\mu_0 m^{*3/2}$ of electrons and holes.

$$S\left(\frac{k_B}{e}\right)^{-1} = \frac{\beta-1}{\beta+1}\ln\sigma + \left[\frac{1-\beta}{1+\beta}\left(\frac{5}{2} + r + ln\frac{2e(2\pi k_B T)^{3/2}}{h^3}\right) + \frac{ln\mu_{h,0}m_h^{*3/2} - \beta ln\mu_{e,0}m_e^{*3/2}}{1+\beta} + \frac{\beta ln\beta + (1-\beta)\ln(1+\beta)}{1+\beta}\right] \quad (1)$$

Here *r* is the scattering exponent, which takes different constant values for different carrier scattering mechanisms.

The case is a bit more complex for bulk samples, which are essentially two-layered structures: a thin, photo-excited-carrier doped top layer; and a much thicker bottom layer with properties unaffected by photons. Previously, when measurements were interpreted with a two-layer model, assumptions had to be made on the top layer thickness and photo-excited carrier densities. This approach didn't provide much

useful insight studying bulk samples. In contrast, we formulated an analysis, with the use of only observable properties, to extract the ratio of electron and hole mobilities β. Different from the thin film case that looked at S vs $\ln\sigma$, for bulk samples S needs to be replaced by $(S\text{-}S_0)\sigma/(\sigma-\sigma_0)$ (S and σ are measured properties under illumination, S_0 and σ_0 are dark properties), and $\ln\sigma$ will be replaced by $\ln I_{ph}$ (I_{ph} is the photon intensity). The relation $(S\text{-}S_0)\sigma/(\sigma\text{-}\sigma_0)$ vs $\ln I_{ph}$ is linear and β can be determined from the slope. The analytical form is given by Eq. 2 (detailed derivation can be found in ref.[32]).

$$(S-S_0)\frac{\sigma}{\sigma-\sigma_0}\left(\frac{k_B}{e}\right)^{-1} = a\frac{\beta-1}{\beta+1}\ln I_{ph} + \left\{\frac{1-\beta}{1+\beta}\left(\frac{5}{2}+r+ln\frac{2e(2\pi k_B T)^{3/2}}{h^3}-ln\phi\right)+\right.$$

$$\left.\frac{3}{2}\frac{ln\mu_h m_h^*-\beta ln\mu_e m_e^*}{1+\beta}+\frac{\beta ln\beta+(1-\beta)\ln(1+\beta)}{1+\beta}\right\}-S_0\left(\frac{k_B}{e}\right)^{-1} \quad (2)$$

In Eq. 2, α and ϕ are parameters determined from the relation between photo-conductivity and photon intensity:

$$\ln(\sigma-\sigma_0) = alnI_{ph} + ln\phi + ln\frac{d}{D+d} \quad (3)$$

D and d are the thickness of bottom layer and top layer, respectively. Their values are treated as unknowns. Only the value of α is needed for analysis, which is determined from the slope of $ln(\sigma\text{-}\sigma_0)$ vs lnI_{ph}.

Eq. 2 is based on general transport theory thus should be valid as long as the following approximations can be justified: 1) photo-excited carrier density distribution at different depths inside a bulk sample is approximated by a uniform density in a top layer. The rest of the sample remain unaffected by photons. This is a commonly used approximation[12, 33], and very close to reality in intrinsic inorganic semiconductors, since absorptions typically happen within 1μm while carrier diffusion length can be 10 to 100 μm. 2) carrier mobilities doesn't change with carrier density. This is seen for many semiconductors[31] including Si, GaAs, GaN and Ga_2O_3 [34] at low carrier

densities. In general, we believe it's a good approximation when around room temperature and low carrier densities ($<10^{16}$ cm^{-3}). The reason is discussed as following: Mobilities are determined by carrier scattering mechanisms. Acoustic phonon scattering, which is often the dominant mechanism, leads to constant mobilities when *n* approaches non-degenerate limit[2]. In fact, it can be shown that this holds for any scattering mechanism, as long as the energy dependence of relaxation time τ can be simplified as $\tau = \tau_0 E^r$,. This is because all Fermi integrals $F_n(E)$ approach *exp(E)* multiplied by constants with E<<0. Ionized impurity scattering leads to more complex relaxation time τ [35] but is not relevant since the samples are intrinsic and no 'ionized impurity'(dopant) is introduced by photons (one exemption is, when large numbers of compensating defects are present). Scatterings from optical phonons[36] (polar and piezoelectric) could have carrier-density dependence, which we found no report to prove or disprove (the temperature dependences are most often studied). Nonetheless, the mobilities are found carrier-density-independent in GaAs and GaN[31], when optical phonon scatterings are known important[37]in these polar, III-V semiconductors. Instead, unintentional variation among samples should be responsible for different mobilities seen at low carrier densities.

Figure 6 demonstrates the application of this analysis to Si. At dark the Si sample has a conductivity of σ_0 = 0.025 S/m, this corresponds to a carrier density of 1.1×10^{12} cm^{-3}. With illumination centered at 565nm and 780nm (both above its bandgap), the photo-Seebeck coefficients are measured with light modulation from a mechanical chopper (1 Hz). This frequency is slow enough for the sample to reach steady-state, hence the modulated illumination is no different from steady illumination for transport properties. The use of modulated illumination will only improve the detectivity of small signal changes. Since the majority of the sample along its thickness direction is unaffected by photons, the observable difference between photo-Seebeck coefficient and the dark Seebeck coefficient is very small. In this experiment shown in Fig. 6, the difference was no more than 4 μV/K (the dark value is S_0 = -1700 μV/K) with 565 nm light source, and 7 μV/K with 780 nm source, respectively. The use of highly sensitive AC measurement technique is essential.

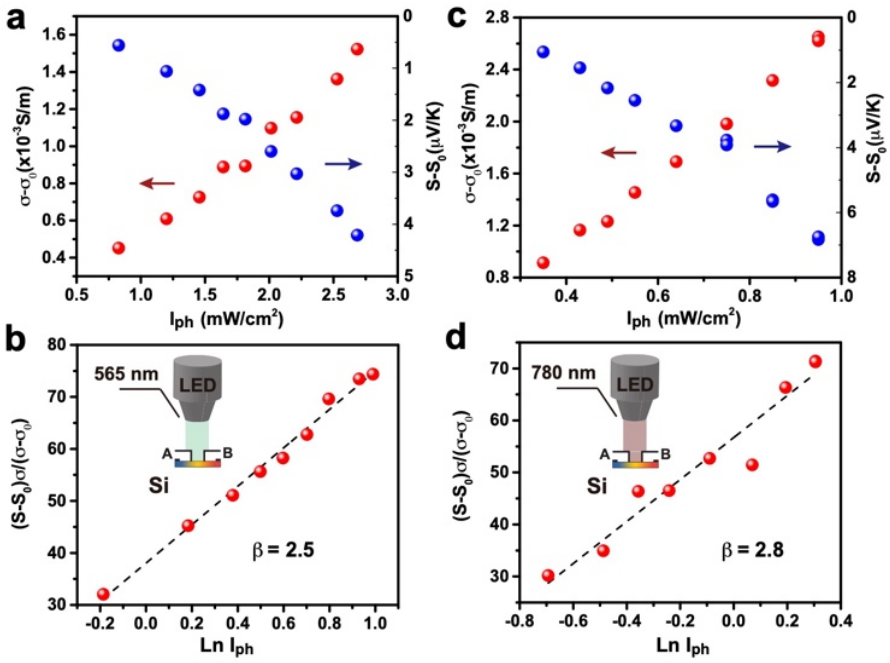

Fig. 6 Mobilities in Si from Photo-Seebeck effect with 565 nm and 780 nm light sources. a), c) change of σ and S as a function of light intensity I_{ph}. b), d) $(S-S_0)\sigma/(\sigma-\sigma_0)$ vs $\ln I_{ph}$ showing a linear relationship, from the slope β is calculated to be 2.5 and 2.8, where the standard ratio is 3. Unit for I_{ph} is mW/cm^2.

For both wavelengths, the relations between $(S-S_0)\sigma/(\sigma-\sigma_0)$ and $\ln I_{ph}$ are found linear, from the slope β is found to be 2.5 and 2.8 with the use of 565 nm and 780 nm LEDs. The two wavelengths lead to essentially the same result, which is expected from our analysis, where photons with wavelengths above band gap are considered no different. The expected value[31] of β for Si is around 3 (generally accepted mobility values are 1450-1500 cm^2/Vs for electrons and450-500 cm^2/Vs for holes). The measured electron mobility from this particular sample is 1470 cm^2/Vs. Thus, our result provides a fairly accurate estimate of the hole mobility and the mobility ratio β. Keep in mind that since β is 'measured' indirectly from relations of three measurements (S, σ, and I_{ph}), it's reasonable to expect an uncertainty that is over 10%.

We performed the same analysis on Se which has a distinctively different photo response due to defect influences. Additional factors have to be taken into account to understand the results. Se is a p type semiconductor with carrier density between[38, 39] 10^{11} and 10^{13} cm^{-3}. For the sample we used, the measured Seebeck coefficient in dark is S_0 = +1250 μV/K, and the conductivity $\sigma_0 = 3.5\text{x}10^{-4}$ S/m. AC measurements were performed with temperature modulation. This will not provide the same sensitivity as illumination modulation but is more accurate than DC methods considering the sample resistance over 1 MΩ. Fortunately, the change in Seebeck coefficient in this case is up to -43 μV/K, significant enough to determine the trend.

Differences from the Si case can be readily noted: first, S decreases with increasing photon intensities whereas for Si S increased (numerical value, not magnitude); second, the curvature of $S - S_0$ vs $\ln I_{ph}$ is also different compared with Si. Despite of the

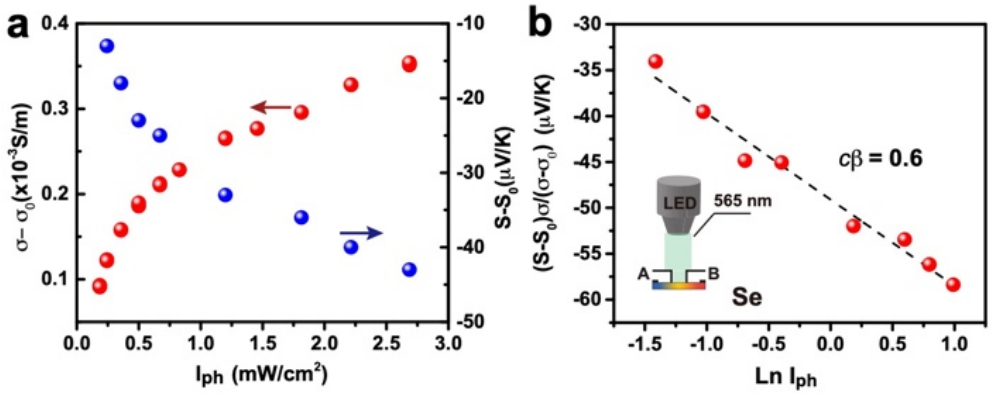

Fig.7 Initial validation using polycrystalline Se. a) change of σ and S as a function of light intensity I_{ph}. b) $(S\text{-}S_0)\sigma/(\sigma-\sigma_0)$ vs $\ln I_{ph}$ showing a linear relationship, from the slope $c\beta$ is calculated to be 0.6. c is a factor introduced due to defect influence (see text). Unit for I_{ph} is mW/cm^2.

differences, when $(S\text{-}S_0)\sigma/(\sigma\text{-}\sigma_0)$ is plotted against lnI_{ph}, a linear trend can also be observed.

β found from the slope based on Eq. 2 is 0.6. Although the possibility can't be ruled out to have electron mobility less than hole mobility, existing example among bulk semiconductors is rare (if any). A re-exam of the theory indicates that photo-Seebeck property in defect-free and defect-rich semiconductors can't be interpreted the same way (the same is true for photo-Hall effect and photo-conductivity). Defect-rich semiconductors posted additional complexity such that photons not necessarily generate equal numbers of free electrons and holes. Defects affect the generation and recombination of excited electrons and holes in various, complex ways. Unequal numbers of free electrons and holes is well-known in historical studies of photo-conductors[40-42]: many early photo-conductors are defective semiconductors and the good photo-sensitivity is mainly contributed by the dominance of only one type of free carriers and the resulted ultra-long carrier lifetimes. Experimentally, slow responses to illumination changes and the dependence of photocurrent on illumination intensity can be used as indications of large numbers of defects, when this is the case, the photo-Seebeck effect along will not be enough to determine β.

Given the similarities in the trend, we believe our analysis can be generalized by assuming a ratio between excited free electrons and holes, which is expressed by $c = \Delta n_e/\Delta n_h$. If the photo-carrier densities change within small ranges relative to the total defect states, c can be taken as constant.

We can show that same relations given by Eq. 1 through 4 still hold, with β replaced by a product $c\beta$. For the case of Se, 0.6 is the value determined for the product $c\beta$. Fortunately, theoretical analysis indicated that individual values of c and β can be solved by combining photo-Seebeck coefficient with another photo-transport property: photo-Hall effect. We are currently working on this experiment. Ultimately, studying the photo-thermoelectric properties could be adopted in high-throughput studies to evaluate mobilities of both electrons and holes at the same time. On the other hand, We expect c to be an important piece of information regarding the defects, as this relative numbers of electrons and holes depends on the defect position in the gap, the filling fraction of defect levels, as well as how effective they are in capturing each type of carriers.

5. Conclusions

We studied photo-Seebeck effect using two distinctively different semiconductors. We found the measured voltages proportional to the temperature difference could come from both a photovoltaic effect at the contact interfaces, and a transport effect due to photo-excited carriers. The latter is the analogue of conventional Seebeck effect and can be understood with classic transport theory. We demonstrated that photo-Seebeck effect in bulk samples can be studied with proper methods. We formulated an analysis, which allowed us to determine the ratio of electron and hole mobilities

from a single sample, with no chemical doping necessary. We demonstrated this on a single crystal Si sample where we found the ratio of mobilities to be 2.5 and 2.8, agree well with established value for Si around 3. When combined with standard Hall effect measurements, mobilities of both carriers are determined. We also discussed the influence of defects on photo-Seebeck properties. Defects create unequal numbers of free electrons and holes. In this case photo-Seebeck effect alone can only determine the product $c\beta$. Nonetheless, when combined with other photo-transport measurements, both c and β can be determined individually. In this regard, photo-Seebeck effect is a powerful tool to study carrier mobilities, as well as influences of defects on free carrier generation and their transport.

Author contributions

Z. P., J. U. and H.W. conceived this research, Z. P. performed the measurements and analysed results, Z. Z. prepared the Se sample. All authors contributed to discussions and finalizing the manuscript.

Competing interests

There are no competing interests to declare.

Acknowledgements

Z. P. and H. W. acknowledge the start-up support fromIllinois Institute of Technology. Work at the Molecular Foundry was supported by the Office of Science, Office of Basic Energy Sciences, of the U.S. Department of Energy and by Lawrence Berkeley National Laboratory under U.S. Department of Energy contract no. DE-AC02-05CH11231.

Notes and references

[1] L. E. Bell, Cooling, heating, generating power, and recovering waste heat with thermoelectric systems. Science 321 (2008) 1457-1461.

[2] Y. I. Ravich, B. A. Efimova, I. A. Smirnov, Semiconducting lead chalcogenides, in: Monographs in semiconductor physics, Plenum Press, New York, 1970, vol. 5.

[3] H. Wang, Z. M. Gibbs, Y. Takagiwa, G. J. Snyder, Tuning bands of PbSe for better thermoelectric efficiency. Energy Environ. Sci. 7 (2014) 804.

[4] Q. Zhu, E. M. Hopper, B. J. Ingram, T. O. Mason, Combined Jonker and Ioffe Analysis of Oxide Conductors and Semiconductors. J. Am. Ceram. Soc. 94 (2011) 187-193.

[5] Z. M. Gibbs, H.-S. Kim, H. Wang, G. J. Snyder, Band gap estimation from temperature dependent Seebeck measurement—Deviations from the 2e|S|maxTmax relation. Appl. Phys. Lett. 106 (2015) 022112.

[6] Y. Pei, A. D. LaLonde, H. Wang, G. J. Snyder, Low effective mass leading to high thermoelectric performance. Energy Environ. Sci. 5 (2012) 7963-7969.

[7] Y. Tang, Z. M. Gibbs, L. A. Agapito, G. Li, H.-S. Kim, Marco B. Nardelli, S. Curtarolo, G. J. Snyder, Convergence of multi-valley bands as the electronic origin of high thermoelectric performance in CoSb3 skutterudites. Nat. Mater. 14 (2015) 1223.

[8] H. Xie, H. Wang, Y. Pei, C. Fu, X. Liu, G. J. Snyder, X. Zhao, T. Zhu, Beneficial Contribution of Alloy Disorder to Electron and Phonon Transport in Half-Heusler Thermoelectric Materials. Adv. Funct. Mater. 23 (2013) 5123-5130.

[9] G. Tan, L.-D. Zhao, F. Shi, J. W. Doak, S.-H. Lo, H. Sun, C. Wolverton, V. P. Dravid, C. Uher, M. G. Kanatzidis, High Thermoelectric Performance of p-Type SnTe via a Synergistic Band Engineering and Nanostructuring Approach. J. Am. Chem. Soc. 136 (2014) 7006-7017.

[10] J. G. Harper, H. E. Matthews, R. H. Bube, Two‐Carrier Photothermoelectric Effects in GaAs. J. Appl. Phys. 41 (1970) 3182-3184.

[11] J. G. Harper, H. E. Matthews, R. H. Bube, Photothermoelectric Effects in Semiconductors: n‐ and p‐Type Silicon. J. Appl. Phys. 41 (1970) 765-770.

[12] R. Okazaki, A. Horikawa, Y. Yasui, I. Terasaki, Photo-Seebeck Effect in ZnO. J. Phys. Soc. Jpn. 81 (2012) 114722.

[13] P. S. Mondal, R. Okazaki, H. Taniguchi, I. Terasaki, Photo-Seebeck effect in tetragonal PbO single crystals. J. Appl. Phys. 114 (2013) 173710.

[14] P. S. Mondal, R. Okazaki, H. Taniguchi, I. Terasaki, Photo-transport properties of Pb2CrO5 single crystals. J. Appl. Phys. 116 (2014) 193706.

[15] X. Xu, N. M. Gabor, J. S. Alden, A. M. van der Zande, P. L. McEuen, Photo-thermoelectric effect at a graphene interface junction. Nano Lett. 10 (2010) 562-566.

[16] D. Sun, G. Aivazian, A. M. Jones, J. S. Ross, W. Yao, D. Cobden, X. Xu, Ultrafast hot-carrier-dominated photocurrent in graphene. Nat. Nanotechnol. 7 (2012) 114-118.

[17] M. Buscema, M. Barkelid, V. Zwiller, H. S. van der Zant, G. A. Steele, A. Castellanos-Gomez, Large and tunable photothermoelectric effect in single-layer MoS2. Nano Lett. 13 (2013) 358-363.
[18] G. Qiu, S. Huang, M. Segovia, P. K. Venuthurumilli, Y. Wang, W. Wu, X. Xu, P. D. Ye, Thermoelectric Performance of 2D Tellurium with Accumulation Contacts. Nano Lett. 19 (2019) 1955-1962.
[19] X. Wang, C. I. Evans, D. Natelson, Photothermoelectric Detection of Gold Oxide Nonthermal Decomposition. Nano Lett. 18 (2018) 6557-6562.
[20] X. Lu, L. Sun, P. Jiang, X. Bao, Progress of Photodetectors Based on the Photothermoelectric Effect. Adv. Mater. 31 (2019) e1902044.
[21] H. J. Queisser, Springer New York, New York, NY, 1985, pp. 1303-1308.
[22] O. Gunawan, S. R. Pae, D. M. Bishop, Y. Virgus, J. H. Noh, N. J. Jeon, Y. S. Lee, X. Shao, T. Todorov, D. B. Mitzi, B. Shin, Carrier-resolved photo-Hall effect. Nature (2019).
[23] I. Hadar, T.-B. Song, W. Ke, M. G. Kanatzidis, Modern Processing and Insights on Selenium Solar Cells: The World's First Photovoltaic Device. Adv. Energy Mater. 9 (2019) 1802766.
[24] T. K. Todorov, S. Singh, D. M. Bishop, O. Gunawan, Y. S. Lee, T. S. Gershon, K. W. Brew, P. D. Antunez, R. Haight, Ultrathin high band gap solar cells with improved efficiencies from the world's oldest photovoltaic material. Nat. Commun. 8 (2017) 682.
[25] J. Treusch, R. Sandrock, Energy Band Structures of Selenium and Tellurium (Kohn-Rostoker Method). Phys. Status Solidi B 16 (1966) 487-497.
[26] H. Yin, A. Akey, R. Jaramillo, Large and persistent photoconductivity due to hole-hole correlation in CdS. Phys Rev. Mater. 2 (2018) 084602.
[27] M. Madel, F. Huber, R. Mueller, B. Amann, M. Dickel, Y. Xie, K. Thonke, Persistent photoconductivity in ZnO nanowires: Influence of oxygen and argon ambient. J. Appl. Phys. 121 (2017) 124301.
[28] J. Tauc, Photo and thermoelectric effects in semiconductors, Pergamon Press, Oxford 1962.
[29] A. Rose, Concepts in photoconductivity and allied problems, Interscience Publishers, Hoboken, 1963.
[30] L. M. Batukova, I. A. Karpovich, Carrier lifetime in single-crystal PbS films. Russ. Phys. J. 13 (1970) 741-743.
[31] Semiconductors on NSM, http://www.ioffe.ru/SVA/NSM/Semicond/index.html, (accessed September 2020).
[32] Z. Pan, Z. Zhu, J. J. Urban, F. Yang, H. Wang, Photo-thermoelectric properties and their use in study of transport properties of both carriers from a single bulk sample. (2019).
[33] R. H. Bube, H. E. MacDonald, J. Blanc, Photo-hall effects in photoconductors. J. Phys. Chem Solids 22 (1961) 173-180.
[34] N. Ma, N. Tanen, A. Verma, Z. Guo, T. Luo, H. Xing, D. Jena, Intrinsic electron mobility limits inβ-Ga2O3. Appl. Phys. Lett. 109 (2016).
[35] D. Chattopadhyay, H. J. Queisser, Electron scattering by ionized impurities in semiconductors. Rev. Mod. Phys. 53 (1981) 745-768.
[36] D. L. Rode, Electron Mobility in Ⅱ- Ⅵ semiconductors. Phys. Rev.B 2 (1970) 4036-4044
[37] H. Ehrenreich, Band Structure and Transport Properties of Some 3–5 Compounds. J. Appl. Phys. 32 (1961) 2155-2166.

［38］ J. Dresner, The photo-hall effect in vitreous selenium∗. J. Phys Chem. Solids 25 (1964) 505-511.
［39］ J. Stuke, K. Wendt, Phonon-Drag in hexagonalen Se-Kristallen. Phys. Status Solidi B 8 (1965) 533-542.
［40］ J. N. Humphrey, R. L. Petritz, Photoconductivity of Lead Selenide: Theory of the Mechanism of Sensitization. Phys. Rev. 105 (1957) 1736-1740.
［41］ R. N. Zitter, Role of Traps in the Photoelectromagnetic and Photoconductive Effects. Phys. Rev. 112 (1958) 852-855.
［42］ M. K. Sheinkman, V. A. Tyagai, O. V. Snitko, I. B. Ermolovich, G. L. Belenky, V. Nbondakenko, Studies on the Nature of CdS Single Crystal Sensitization by Etching. Phys. Status Solidi B 24 (1967) 543-549.